Main component of soft tissue artifact of the upper-limbs with respect to different functional, daily life and sports movements.

Yoann Blache, Raphaël Dumas, Arian Lundberg, Mickaël Begon

To cite this version:

Yoann Blache, Raphaël Dumas, Arian Lundberg, Mickaël Begon. Main component of soft tissue artifact of the upper-limbs with respect to different functional, daily life and sports movements.. Journal of Biomechanics, 2017, 62, pp.39-46. 10.1016/j.jbiomech.2016.10.019 . hal-01627925

www.elsevier.com/locate/jbiomech

Main component of soft tissue artifact of the upper-limbs with respect to different functional, daily life and sports movements

Y. Blache, R. Dumas, A. Lundberg, M. Begon

PII: S0021-9290(16)31115-0
DOI: http://dx.doi.org/10.1016/j.jbiomech.2016.10.019
Reference: BM7929

To appear in: *Journal of Biomechanics*
Accepted date: 2 October 2016

Cite this article as: Y. Blache, R. Dumas, A. Lundberg and M. Begon, Main component of soft tissue artifact of the upper-limbs with respect to different functional, daily life and sports movements, *Journal of Biomechanics* http://dx.doi.org/10.1016/j.jbiomech.2016.10.019

Main component of soft tissue artifact of the upper-limbs with respect to different functional, daily life and sports movements

Blache Y [1,2], Dumas R [4], Lundberg A[5], Begon M [2,3]

[1] Université de Lyon, université Lyon 1, Laboratoire Interuniversitaire de Biologie de la motricité, Villeurbanne, France
[2] Laboratoire de Simulation et Modélisation du Mouvement, Département de Kinésiologie, Université de Montréal, Montréal, QC, Canada
[3] Centre de Recherche du Centre Hospitalier Universitaire Sainte-Justine, Montréal, QC, Canada
[4] Université de Lyon, F-69622, Lyon; IFSTTAR, LBMC, UMR_T9406, Bron; Université Lyon 1, Villeurbanne, France
[5] Karolinska Institute, Stockholm, Sweden

Corresponding author

Blache Yoann

Université de Lyon, université Lyon 1, Laboratoire Interuniversitaire de Biologie de la motricité, Villeurbanne, France

E-mail: yoann.blache@univ-lyon1.fr

Tel: +33 4 72 43 28 43

Key words: skin marker; geometrical transformation; cluster deformation; deformation energy; shoulder complex

Abstract

Soft tissue artifact (STA) is the main source of error in kinematic estimation of human movements based on skin markers. Our objective was to determine the components of marker displacements that best describe STA of the shoulder and arm (*i.e.* clavicle, scapula and humerus). Four participants performed arm flexion and rotation, a daily-life and a sports movement. Three pins with reflective markers were inserted into the clavicle, scapula and humerus. In addition, up to seven skin markers were stuck on each segment. STA was described with a modal approach: individual marker displacements or marker-cluster (*i.e.* translations, rotations, homotheties and stretches) relative to the local segment coordinate system defined by markers secured to the pins. The modes were then ranked according to the percentage of total STA energy that they explained. Both individual skin marker displacements and marker-cluster geometrical transformations were task-, location-, segment- and subject-specific. However, 85% of the total STA energy was systematically explained by the rigid transformations (*i.e.* translations and rotations of the marker-cluster). In conclusion, large joint dislocations and limited efficiency of least squares bone pose estimators are expected for the computation of upper limb joint kinematics from skin markers. Future developments shall consider the rigid transformations of marker-clusters in the implementation of an STA model to reduce its effects on kinematics estimation.

Introduction

The assessment of human body kinematics is essential in many research fields such as orthopedics, ergonomics and sport biomechanics. Accuracy of the skeleton pose estimate is dependent of the methods used to record body kinematics. Usually, trajectories of reflective markers stuck on the skin are recorded using stereophotogrammetry. Nevertheless, skin marker trajectories are affected by the soft tissue artifact (STA) defined as the relative movement between each skin marker and its underlying bone (Leardini et al., 2005; Peters et al., 2010). Since STA representations vary among literature, Dumas et al. (2014a) have proposed a generalized mathematical representation of the STA: individual marker displacements, marker-cluster geometrical transformations and skin envelope shape variations. Among these three representations, STA are more usually described either by individual marker displacements or marker-cluster geometrical transformations (Alexander and Andriacchi, 2001; Andriacchi et al., 1998; Benoit et al., 2015; Dumas and Cheze, 2009).

The ultimate purpose of STA assessment is to implement methods in order to improve kinematics estimation. These methods can be used either to define mathematical models that can be embedded in optimal bone pose estimator (Alexander and Andriacchi, 2001; Bonci et al., 2014; Camomilla et al., 2015; Camomilla et al., 2013), to implement functional algorithms for locating joint rotation center (De Rosario et al., 2013) or to assess the dynamic effects of the wobbling mass (Bélaise et al., 2016; Thouze et al., 2015). As STA may not be defined *a priori* because they are subject-, task- and segment-specific, a calibration (*i.e.* identification of the components that define the STA and of the parameters that model these components) is necessary for each studied movement. Consequently, some studies aimed at describing the components, among individual marker displacements or marker-cluster geometrical transformations that best describe STA. These studies have been performed exclusively concerning the lower-limb STA. Briefly, these investigations pointed out which skin markers located on the thigh and shank were the most subject to the STA (Akbarshahi et al., 2010; Dumas et al., 2014b; Kuo et al., 2011; Tsai et al., 2011). In addition, it was observed that STA of the lower limbs were mainly explained by rigid transformations (*i.e.* translations and rotations) and in a less manner by deformations (*i.e.* homotheties and stretches) of the marker-cluster (Andersen et al., 2012; Barre et al., 2015; Barre et al., 2013; Benoit et al., 2015; Benoit et al., 2006; de Rosario et al., 2012; Dumas et al., 2014b; Grimpampi et al., 2014). Although many studies give either qualitative or quantitative information about STA for the lower limbs, no data is available in the literature concerning the characterization of the STA for the upper-limb.

The objective of this study was to describe the main components that best represent the STA of the shoulder complex and arm during functional arm movements and daily-life or sports movements. Firstly, the description of the displacement of the individual skin markers was analyzed. Secondly, special consideration was given to the analysis of marker-cluster geometrical transformations. To that purpose, the trajectories of the skin markers relative to the bone were computed using reflective markers secured to intra-cortical pins. As STA has been shown to be task-specific, the analysis focused on movements with different amplitudes, degrees of freedom and velocities. To that aim, arm flexions and rotations as well as hair combing and hockey shooting were investigated. According the studies about the STA of the lower limb, it was hypothesized, that the STA energy was task-, location- segment- and subject-specific, while the rigid transformations of the marker-cluster explained the main part of the STA energy.

1. Methods

1.1. Participants

The raw data obtained by Dal Maso et al. (2014) have been used in this study. Four healthy male participants (age ranged between 27 and 41 years, mass ranged between 57 and 115 kg, height ranged between 1.65 and 1.82 m) volunteered to participate in this study. They signed an informed consent which was approved by the Karolinska Institute (Sweden) and the University of Montreal (Canada) ethics committees. None of the participants presented current or previous shoulder injuries.

1.2. Instrumentation

Four or five reflective markers secured to pins were respectively inserted into the first third of the scapula spine and the clavicle, and below the attachment of the medial deltoid on the humerus. The pin locations were chosen to avoid muscles such that the movement pattern remained unchanged. They were also oriented to avoid contacts between markers and head or neck during movements (see Dal Maso et al. (2014) for details about the surgical insertion). In line with the kinematic shoulder model of Jackson et al. (2012), 16 skin markers were placed on the left clavicle (5), scapula (4), upper arm (7) (Fig. 1). Marker trajectories for each movement were measured with an 18-camera optoelectronic VICON^{TM} system (T-40S and T-20S; Oxford Metrics Ltd., Oxford, UK) sampled at 300 Hz. The experiment was conducted under local anaesthesia that lasted two hours.

Insert Figure 1 near here

1.3. Procedures

Prior to the test, participants held for a few seconds an anatomical and then a rest static positions. Thereafter they performed functional movements, including arm flexion, rotation and circumduction. This procedure was used to determine joint centre of rotations and to define segment coordinate system for the STA description (see section 2.4.). The movements of interest were two kind of functional movements performed up to 11 repetitions; they consisted in arm flexions (i.e. elevation in the sagittal plane) and arm rotations with the arm at 0° and 90° of abduction (with maximal range of motion). For the arm flexion, participants had to keep a neutral internal/external arm rotation, and the elbow extended throughout the movements. Nevertheless because of the discomfort induced by the humeral pin, the second participant performed only two trials of arm flexion. Concerning the arm rotations, participants had to keep their elbow at 90° of flexion throughout the movement. In addition, the participants performed six trials of a daily-life activity (i.e. to mimic hair combing) and a sport movement (i.e. to mimic hockey shooting with a hockey stick). The participants performed their movements at their preferred speed.

1.4. Data Processing

Joint center of rotation locations were obtained from the functional symmetrical centre of rotation algorithm (Ehrig et al., 2006) implemented with pin markers. Skin markers and joint center of rotation locations obtained during the static position were used to define each segment coordinate system according to the ISB (Wu et al., 2005) and Jackson et al. (2012) recommendations. Joint angles were computed using a single-body kinematic optimization algorithm, consisting in minimizing the quadratic Euclidean distance between the experimental pin markers and virtual markers of the kinematic model. Finally, the skin marker displacements were expressed with respect to their underlying segment coordinate system.

Finally, the helical axis angle between the orientations of the pin- and skin-based local coordinate systems was calculated at the beginning of each trial in order to assess a possible rotation of the markers support on the pin or pin loosening. A drift of this angle for the scapula of two participants was identified after a few trials. Consequently the data concerning the scapula were removed for these two participants.

1.5. Soft tissue artifact

From pin and skin markers, the method developed by Dumas et al. (2014a) was implemented to describe STA relative to the scapula, clavicle and humerus. Briefly, STA fields $\mathbf{V}_i\ (k)$ were computed to represent the displacements that all skin markers $\{1, \dots, m_i\}$ associated with the segment $i \in \{1, \dots, 3\}$ undergoes relative to the segment coordinate system at each sampled instant of time $k \in \{1, \dots, n\}$ from a reference position defined during the static posture. STA fields were then represented by a series of modes (*l*):

$$\mathbf{V}_i(k) = \sum_{l=1}^{3m_i} a_i^l\,(k)\boldsymbol{\Phi}_i^l\ , \tag{1}$$

where $a_i^l(k)$ corresponds to the amplitude of the projection of $\mathbf{V}_i(k)$ onto the basis vector $\boldsymbol{\Phi}_i^l$ and can be obtained as follow:

$$a_i^l(k) = \left(\mathbf{V}_i(k)\right)^T \cdot \boldsymbol{\Phi}_i^l \tag{2}$$

The definition of the basis vectors $\boldsymbol{\Phi}_i^l$ for both individual skin marker displacements and marker-cluster geometrical transformations (i.e. translations, rotations, homotheties and stretches) is detailed in Dumas et al. (2014a). Finally, the modes were ranked by computing the STA energy:

$$\lambda_i^l = \frac{1}{n}\sum_{k=1}^{n}\left(a_i^l(k)\right)^2. \tag{3}$$

Note that the total STA energy is the sum of the above mentioned modal ones.

1.6. Analyzed variables

Firstly, the upper-limb STA were described by the analysis of the individual skin marker displacements, which corresponded to the modes in Eq.1. The percentage of the total STA energy explained by each individual marker displacement along its three dimensional axis was calculated. Then, to enable a global analysis, the STA energies of the three dimensional axis of a given skin marker were summed.

Secondly, the upper-limb STA have been defined as marker-cluster geometrical transformations, which corresponded to the modes in Eq.1 (i.e., translations, rotations, homotheties and stretches along the three dimensional axis). Similarly as for individual skin marker displacements, the STA energies of the three dimensional axis for a given geometrical transformation were summed.

Finally, the analyzed variables cited above have been calculated for each trial (up to 11) of each movement. Then the mean value of the trials for a given movement (arm flexion or rotation; hair combing; or hockey shooting) and a segment (clavicle, scapula and humerus) were considered for the analysis. Due to the small number of subjects, no statistics was performed.

2. Results

First of all, as the pin inserted into the scapula rotated a few degrees for two participants, the data concerning the scapula were given for only two remaining participants. The joint angles of each movement computed with the pin markers were presented in figure 2. The durations of the movements were 3.63±1.16 s, 1.57±0.31 s, 1.34±0.45 s and 0.94±0.54 s for the arm flexion/extension, arm rotation, combing mimic and hockey shooting mimic respectively.

2.1. Individual skin marker displacements

The relative percentage of total STA energy explained by each marker varied among participants and motions. Nevertheless some similitude may be noticed. Concerning the clavicle, the markers CL1 and CL4 represented the greatest percentages of the total STA energy (31% on average for each marker), but for the hockey shooting. Indeed for the latter movement CL2 energy was significantly greater than the CL4 one (Fig. 3). Concerning the scapula, it appeared that each marker would have a similar contribution to the total STA energy for the rotation and hair-combing movements. By contrast SS1 and SS2 had the greatest percentages of total STA energy for the flexion and hockey-shooting movements (Fig. 3).

Concerning the humerus, during the flexion movement, the markers Tri2, Bic1 and Bic2 generally explained the greatest part of the total STA energy (23% on average for each marker), while EpM and EpL were the markers that presenting the less STA energy (5% on average for each marker) (Fig. 3). For the rotation and hair-combing movements, Tri2 and EpL explained most of the time the greatest part of total STA energy (25% on average for each marker) (Fig. 3). Finally, for the hockey-shooting similar percentage of STA energy was observed between each marker (Fig. 3).

Insert Figure 2 near here

2.2. Marker-cluster geometrical transformations

Concerning the clavicle, the translation of the marker-cluster explained the greatest percentage of the total STA energy in three participants (60% on average). Similar percentages were observed between the rotation and homothety, while the smallest percentage of the total STA energy was observed for the stretch (Fig. 4). Concerning the scapula, it seemed that the translation of the marker-cluster explained also the greatest percentage of total STA energy. For the humerus, during the arm flexion movement the translation of the marker-cluster represented the greatest percentage of the total STA energy (66% on average), followed by the arm rotation and stretch, while the homothety represented the smallest percentage (Fig. 4). Concerning the rotation and hair-combing movements, the total STA energy was explained in a descending order by rotation (53% on average), translation, homothety and stretch of the marker-cluster (Fig. 4). Finally, for the hockey-shooting, the rigid transformations (translation and rotation) represented a similar percentage of total STA energy (37% on average for each mode), that was greater than the homothety and stretch (Fig. 4).

Insert Figure 3 near here

When the rigid transformations were summed and compared to the sum of the non-rigid transformations, the sum of rigid transformations always explained the greatest part of the total STA energy (on average 85% of the total STA energy), regardless the segment and the movement and the participant.

Insert Figure 4 near here

3. Discussion

The purpose of this study was to describe the main components that best describe the STA of the shoulder complex and arm during functional arm movements and daily-life or sports movements. To that aim, the percentage of the total STA energy explained either by individual marker displacements or marker-cluster geometrical transformations was computed. Our hypotheses were confirmed since we firstly observed that the individual marker displacements were task- location- and subject-specific. Secondly, concerning the marker-cluster geometrical transformations, the rigid part systematically explained at least 85% of the total STA energy regardless the task and the segment. However, the proportion of translation and rotation was different with regards to the segment, task and participant.

3.1. Limits

Our results were observed on a small sample size, consequently further studies using fluoroscopy or intra cortical pins with more participants are needed to confirm our conclusions. Nevertheless, it can be noticed, that the statistical methods used, enabled to perform mixed-linear model analysis on small samples (Leys 2010) and showed excellent statistical power (superior to 0.9). The second limit was that the displacements of the skin marker located near to the pins may have been slightly reduced, since the skin may present less movement in this area. The third limit was that the subjects could only mimic daily-living and sport movements, especially because of the environmental context, which may not totally reflect movements with strong impacts. The fourth limit was that we used the definition given by Dumas et al. (2014a) to describe the geometrical transformations, while alternative definitions are also given in the literature (Andersen et al., 2012; Barre et al., 2013; de Rosario et al., 2012; Grimpampi et al., 2014). Nevertheless the definition of Dumas et al. (2014a) has been used in several studies investigating the STA of the lower limbs (Camomilla et al., 2015; Dumas et al., 2014b, 2015) which, showed similar results for the lower limb as studies using other definitions. Finally, the metric used to describe the main components of the STA was the percentage of total energy. This is not widely used in biomechanics, nevertheless this metrics has been used in study about the STA of the lower limbs (Camomilla et al., 2015; Dumas et al., 2014b) and is very similar in principle to the fraction of total STA magnitudes as proposed by Benoit et al. (2015).

3.2. Individual skin marker displacements

The Individual skin marker displacement of the present study seemed to be subject-, task- and location-specific. These results generalize the findings observed for the humerus (Begon et al., 2015), the scapula (Matsui et al., 2006) and the lower limbs (Akbarshahi et al., 2010; Andersen et al., 2012) to the whole shoulder complex. Nevertheless, regardless the task and participant, some markers such as CL5 (lateral part of the clavicle) and EpM (medial epicondyle of the humerus) were always few affected by STA. Consequently as suggested by Begon et al. (2015) these marker locations (lateral part of the clavicle and medial epicondyle of the humerus) may be relevant for a set using a limited number of markers or when the experimenter looks for a sensor location with small STA. Concerning the scapula, (Matsui et al., 2006) observed similar deviation for the two markers located near the acromion process, while the skin marker located on the inferior angle underwent the highest deviation. We studied only skin markers located near the acromion process, which may explain why none of our scapula markers presented more or less STA.

To summarize, when STA is assessed through individual skin marker displacements, even if some markers seemed to be almost STA free, for most of them, STA were subject- and task-specific. In addition, almost no marker represented more than 50% of the total STA energy; by contrast lots of them explained a similar part of the total STA energy. Therefore, we may suggest that none of the skin markers used in this study should be specifically selected or removed when one want to estimate upper-limb kinematics with skin markers.

3.3. Marker-cluster geometrical transformations

As already observed for the lower limbs (Andersen et al., 2012; Barre et al., 2015; Benoit et al., 2015; Dumas et al., 2014b), the marker-cluster geometrical transformations of the upper-limb were task-, segment- and subject-specific. Nevertheless for the clavicle a similar ranking was observed among the four analyzed task namely, the greatest part of the total STA energy was often explained by the translation of the marker-cluster, followed by a similar contribution of the rotation and homothety. Similar results were observed for the scapula. Concerning the humerus translation and rotation explained the greatest part of the total STA energy but for arm flexion task. Interestingly, the highest proportion of maker-cluster translation was specific of this flexion task.

However, although differences were observed among the segment and analyzed movements, the rigid transformations (translation + rotation) summed together always explained a greater part of the total STA energy than the non-rigid transformations (homothety + stretch). On average 85% of the total STA energy was explained by the rigid transformations. These results confirmed those observed on the lower-limbs when rigid and non-rigid transformations were compared during walking (Andersen et al., 2012; Barre et al., 2015; Barre et al., 2013; Benoit et al., 2015), running (Dumas et al., 2014b), cutting manoeuver and hopping (Andersen et al., 2012; Benoit et al., 2015). The upper limb specificity appears in the proportion of marker-cluser rotation at the humerus for most of the movements analysed. Nevertheless, as for the lower limb, least squares bone pose estimators, that compensate only for the non-rigid transformations of the marker cluster, can hardly improve the estimation of joint kinematics, in particular for the shoulder joint (Begon et al., 2015). The large proportion of marker-cluster translation also suggests joint dislocation or inter-penetration if the joint displacements are computed from the skin markers.

Previous studies (Camomilla et al., 2015; De Rosario et al., 2013) investigating the STA of the lower limb have shown that the development of models composed of STA rigid components represents a potential solution for STA compensation. This solution could be extended for the STA compensation in the upper limb. Our study was the first step (i.e. determine the main components that best describe the STA) necessary to implement STA models that may enable to reduce shoulder kinematics errors. The next step will be to consider these rigid transformations in the implementation of a STA model in order to reduce its effects on kinematics estimation. Meanwhile, using a redundant marker set with multibody kinematic optimisation algorithms may currently represent the best method for clinicians and researchers. The accuracy of this method relies on the definition of joint models.

4. Conclusion

Although some studies (Begon et al., 2015; Hamming et al., 2012) assessed the effect of STA on shoulder and upper limb kinematics, to our knowledge, our study was the first one to describe the STA of the shoulder complex (clavicle, scapula and humerus) and may be a benchmark of larger scale study. Our study was performed in a modelling perspective. STA was found task-, location- and subject-specific when analyzing the individual skin marker displacements. Consequently considering individual marker displacements for further development of STA models may be compromised. By contrast, although maker-cluster geometrical transformations were also task-, segment and subject-specific, the rigid transformations explained on average 85% of the total STA energy for all subjects, with a large proportion of maker-cluster translation except for the humerus. Therefore, as for the lower limb that was more widely studied, large joint dislocations and limited efficiency of least squares bone pose estimators can be expected for the computation of joint kinematics from skin markers. New compensation methods addressing the STA rigid component need to be further developed and evaluated.

Conflict of interest statement

None of the authors are in conflict of interest with regards to this research.

References

Akbarshahi, M., Schache, A.G., Fernandez, J.W., Baker, R., Banks, S., Pandy, M.G., 2010. Non-invasive assessment of soft-tissue artifact and its effect on knee joint kinematics during functional activity. Journal of biomechanics 43, 1292-1301.

Alexander, E.J., Andriacchi, T.P., 2001. Correcting for deformation in skin-based marker systems. Journal of biomechanics 34, 355-361.

Andersen, M.S., Damsgaard, M., Rasmussen, J., Ramsey, D.K., Benoit, D.L., 2012. A linear soft tissue artefact model for human movement analysis: proof of concept using in vivo data. Gait & posture 35, 606-611.

Andriacchi, T.P., Alexander, E.J., Toney, M.K., Dyrby, C., Sum, J., 1998. A point cluster method for in vivo motion analysis: applied to a study of knee kinematics. Journal of biomechanical engineering 120, 743-749.

Barre, A., Jolles, B.M., Theumann, N., Aminian, K., 2015. Soft tissue artifact distribution on lower limbs during treadmill gait: Influence of skin markers' location on cluster design. Journal of biomechanics 48, 1965-1971.

Barre, A., Thiran, J.P., Jolles, B.M., Theumann, N., Aminian, K., 2013. Soft tissue artifact assessment during treadmill walking in subjects with total knee arthroplasty. IEEE transactions on bio-medical engineering 60, 3131-3140.

Begon, M., Dal Maso, F., Arndt, A., Monnet, T., 2015. Can optimal marker weightings improve thoracohumeral kinematics accuracy? Journal of biomechanics 48, 2019-2025.

Bélaise, C., Blache, Y., Thouzé, A., Monnet, T., Begon, M., 2016. Effect of wobbling mass modeling on joint dynamics during human movements with impacts. Multibody System Dynamics, 1-22.

Benoit, D.L., Damsgaard, M., Andersen, M.S., 2015. Surface marker cluster translation, rotation, scaling and deformation: Their contribution to soft tissue artefact and impact on knee joint kinematics. Journal of biomechanics 48, 2124-2129.

Benoit, D.L., Ramsey, D.K., Lamontagne, M., Xu, L., Wretenberg, P., Renström, P., 2006. Effect of skin movement artifact on knee kinematics during gait and cutting motions measured in vivo. Gait & posture 24, 152-164.

Bonci, T., Camomilla, V., Dumas, R., Cheze, L., Cappozzo, A., 2014. A soft tissue artefact model driven by proximal and distal joint kinematics. Journal of biomechanics 47, 2354-2361.

Camomilla, V., Bonci, T., Dumas, R., Chèze, L., Cappozzo, A., 2015. A model of soft tissue artefact rigid component. Journal of biomechanics 48, 1752-1759.

Camomilla, V., Cereatti, A., Cheze, L., Cappozzo, A., 2013. A hip joint kinematics driven model for the generation of realistic thigh soft tissue artefacts. Journal of biomechanics 46, 625-630.

Dal Maso, F., Raison, M., Lundberg, A., Arndt, A., Begon, M., 2014. Coupling between 3D displacements and rotations at the glenohumeral joint during dynamic tasks in healthy participants. Clinical biomechanics 29, 1048-1055.

de Rosario, H., Page, A., Besa, A., Mata, V., Conejero, E., 2012. Kinematic description of soft tissue artifacts: quantifying rigid versus deformation components and their relation with bone motion. Medical & biological engineering & computing 50, 1173-1181.

De Rosario, H., Page, A., Besa, A., Valera, A., 2013. Propagation of soft tissue artifacts to the center of rotation: a model for the correction of functional calibration techniques. Journal of biomechanics 46, 2619-2625.

Dumas, R., Camomilla, V., Bonci, T., Cheze, L., Cappozzo, A., 2014a. Generalized mathematical representation of the soft tissue artefact. Journal of biomechanics 47, 476-481.

Dumas, R., Camomilla, V., Bonci, T., Cheze, L., Cappozzo, A., 2014b. A qualitative analysis of soft tissue artefact during running. Computer methods in biomechanics and biomedical engineering 17 Suppl 1, 124-125.

Dumas, R., Camomilla, V., Bonci, T., Cheze, L., Cappozzo, A., 2015. What portion of the soft tissue artefact requires compensation when estimating joint kinematics? Journal of biomechanical engineering 137, 064502.

Dumas, R., Cheze, L., 2009. Soft tissue artifact compensation by linear 3D interpolation and approximation methods. Journal of biomechanics 42, 2214-2217.

Ehrig, R.M., Taylor, W.R., Duda, G.N., Heller, M.O., 2006. A survey of formal methods for determining the centre of rotation of ball joints. Journal of biomechanics 39, 2798-2809.

Grimpampi, E., Camomilla, V., Cereatti, A., de Leva, P., Cappozzo, A., 2014. Metrics for describing soft-tissue artefact and its effect on pose, size, and shape of marker clusters. IEEE transactions on bio-medical engineering 61, 362-367.

Hamming, D., Braman, J.P., Phadke, V., LaPrade, R.F., Ludewig, P.M., 2012. The accuracy of measuring glenohumeral motion with a surface humeral cuff. Journal of biomechanics 45, 1161-1168.

Jackson, M., Michaud, B., Tetreault, P., Begon, M., 2012. Improvements in measuring shoulder joint kinematics. Journal of biomechanics 45, 2180-2183.

Kuo, M.Y., Tsai, T.Y., Lin, C.C., Lu, T.W., Hsu, H.C., Shen, W.C., 2011. Influence of soft tissue artifacts on the calculated kinematics and kinetics of total knee replacements during sit-to-stand. Gait & posture 33, 379-384.

Leardini, A., Chiari, L., Della Croce, U., Cappozzo, A., 2005. Human movement analysis using stereophotogrammetry. Part 3. Soft tissue artifact assessment and compensation. Gait & posture 21, 212-225.

Matsui, K., Shimada, K., Andrew, P.D., 2006. Deviation of skin marker from bone target during movement of the scapula. Journal of orthopaedic science : official journal of the Japanese Orthopaedic Association 11, 180-184.

Peters, A., Galna, B., Sangeux, M., Morris, M., Baker, R., 2010. Quantification of soft tissue artifact in lower limb human motion analysis: a systematic review. Gait & posture 31, 1-8.

Thouze, A., Monnet, T., Belaise, C., Lacouture, P., Begon, M., 2015. A chain kinematic model to assess the movement of lower-limb including wobbling masses. Computer methods in biomechanics and biomedical engineering, 1-10.

Tsai, T.Y., Lu, T.W., Kuo, M.Y., Lin, C.C., 2011. Effects of soft tissue artifacts on the calculated kinematics and kinetics of the knee during stair-ascent. Journal of biomechanics 44, 1182-1188.

Wu, G., van der Helm, F.C., Veeger, H.E., Makhsous, M., Van Roy, P., Anglin, C., Nagels, J., Karduna, A.R., McQuade, K., Wang, X., Werner, F.W., Buchholz, B., International Society of, B., 2005. ISB recommendation on definitions of joint coordinate systems of various joints for the reporting of human joint motion--Part II: shoulder, elbow, wrist and hand. Journal of biomechanics 38, 981-992.

Acknowledgement

This work was partially funded by the NSERC discovery (#RGPIN-2014-03912) grant. The first author is scholar of the Méditis program (NSERC, CREATE).

Figure captions

Figure 1. Picture of the set of skin and pin markers used to determine soft tissue artifact.

Figure 2. Shoulder kinematics of a representative participant with respect to the time for the flexion movement (A), rotation (B), hair combing (C) and hockey shooting (D). For the sternoclavicular joint the protraction(-)/retraction(+), elevation(+)/depression(-) and posterior(-)/anterior(+) rotation are represented by the solid black, dashed black and grey lines respectively. Concerning the acromioclavicular joint the internal(-)/external(+) rotation, upward(+)/downward(-) rotation and anterior(-)/posterior(+) tilt are represented by the solid black, dashed black and grey lines respectively. For the glenohumeral joint the plane of elevation, elevation and the internal(-)/external(+) axial rotation are represented by the black, dashed black and grey lines respectively.

Figure 3. Percentage of total STA energy explained by each individual skin marker displacement according to each segment (left-right) and movement (up-down) for each participant (black: participant 1, dark grey: participant 2, light grey: participant 3, white: participant 4). Refer to figure 1 for the definition of the markers.

Figure 4. Percentage of total STA energy explained by each type of rigid (translation [T] and rotation [R]) and non-rigid (homothety [H] and stretch [S]) transformation as a function of the segment (left-right) and movement (up-down) for each participant (black: participant 1, dark grey: participant 2, light grey: participant 3, white: participant 4).

Figure 1

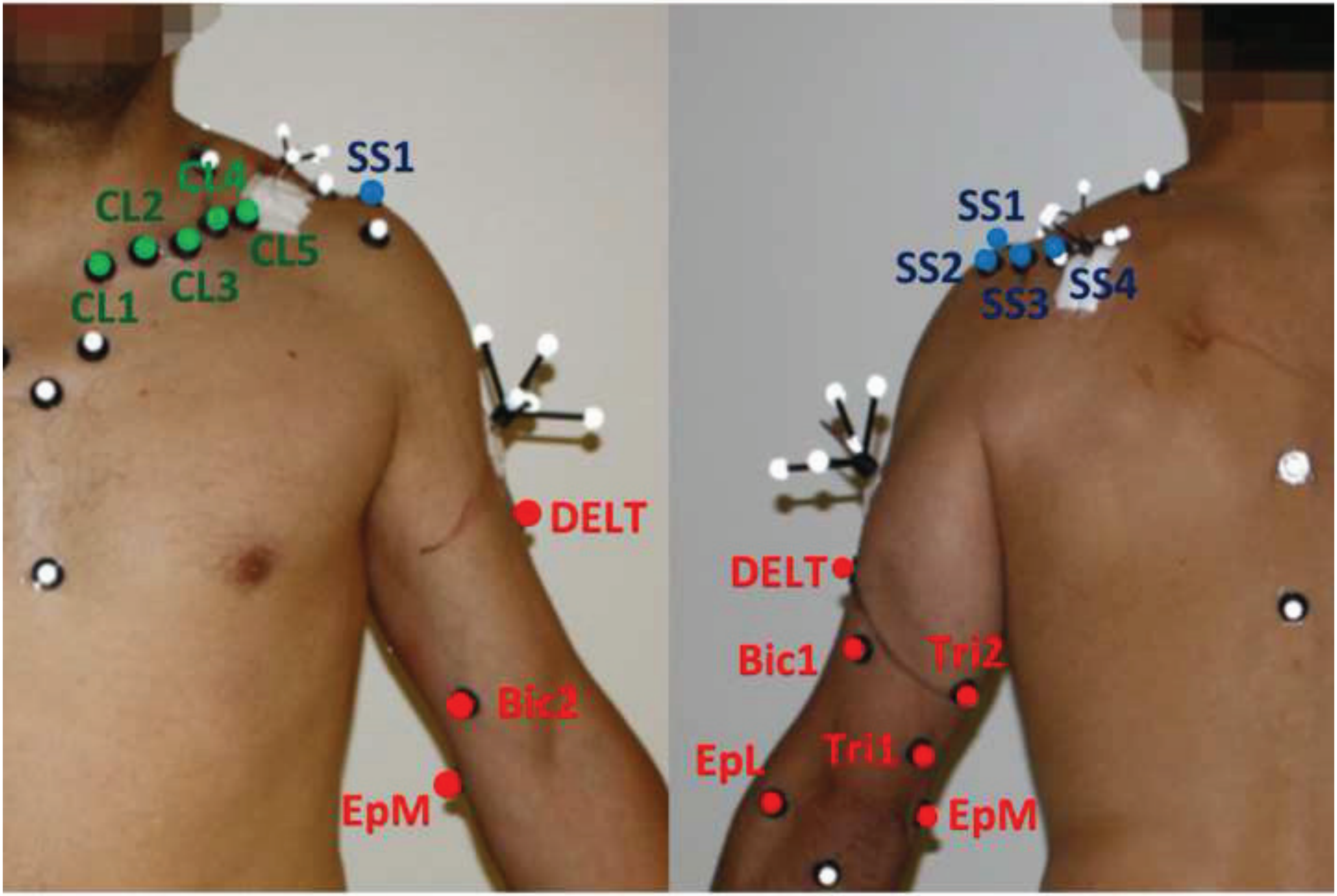
SS1
CL4
CL2
CL5
CL3
CL1
DELT
Bic2
EpM
SS1
SS2
SS3
SS4
DELT
Bic1
Tri2
EpL
Tri1
EpM

Figure 2

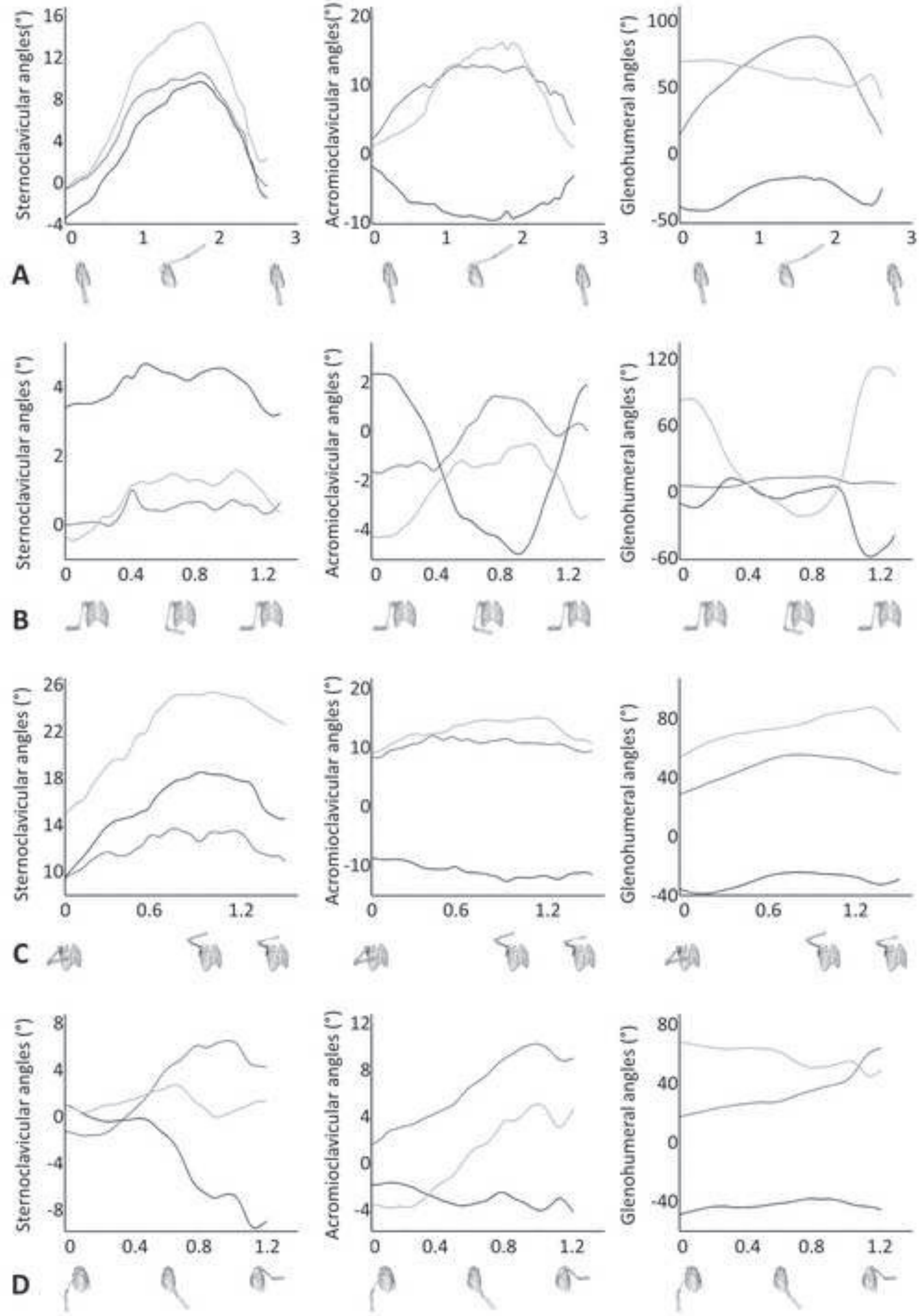
A
B
C
D
Sternoclavicular angles(°)
16
12
8
4
0
-4
0
1
2
3
Acromioclavicular angles(°)
20
10
0
-10
Glenohumeral angles (°)
100
50
0
-50
Sternoclavicular angles (°)
4
2
0
0.4
0.8
1.2
Acromioclavicular angles (°)
2
0
-2
-4
Glenohumeral angles (°)
120
60
0
-60
Sternoclavicular angles (°)
26
22
18
14
10
0.6
1.2
Acromioclavicular angles (°)
20
10
0
-10
Glenohumeral angles (°)
80
40
0
-40
Sternoclavicular angles (°)
8
4
0
-4
-8
Acromioclavicular angles (°)
12
8
4
0
-4
Glenohumeral angles (°)
80
40
0
-40

Figure 3

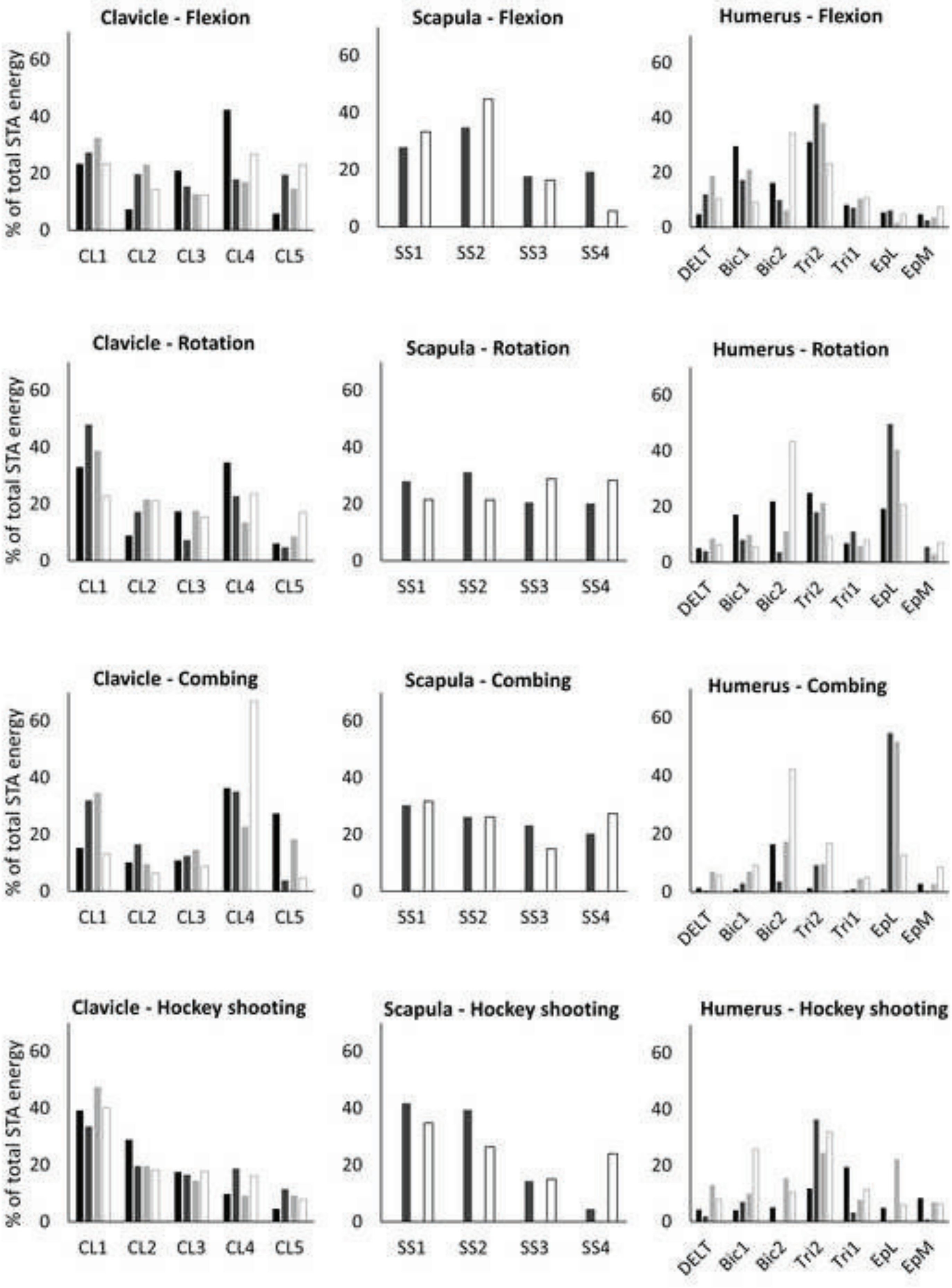
Clavicle - Flexion
Scapula - Flexion
Humerus - Flexion
Clavicle - Rotation
Scapula - Rotation
Humerus - Rotation
Clavicle - Combing
Scapula - Combing
Humerus - Combing
Clavicle - Hockey shooting
Scapula - Hockey shooting
Humerus - Hockey shooting
% of total STA energy
0
20
40
60
CL1
CL2
CL3
CL4
CL5
SS1
SS2
SS3
SS4
DELT
Bic1
Bic2
Tri2
Tri1
EpL
EpM

Figure 4

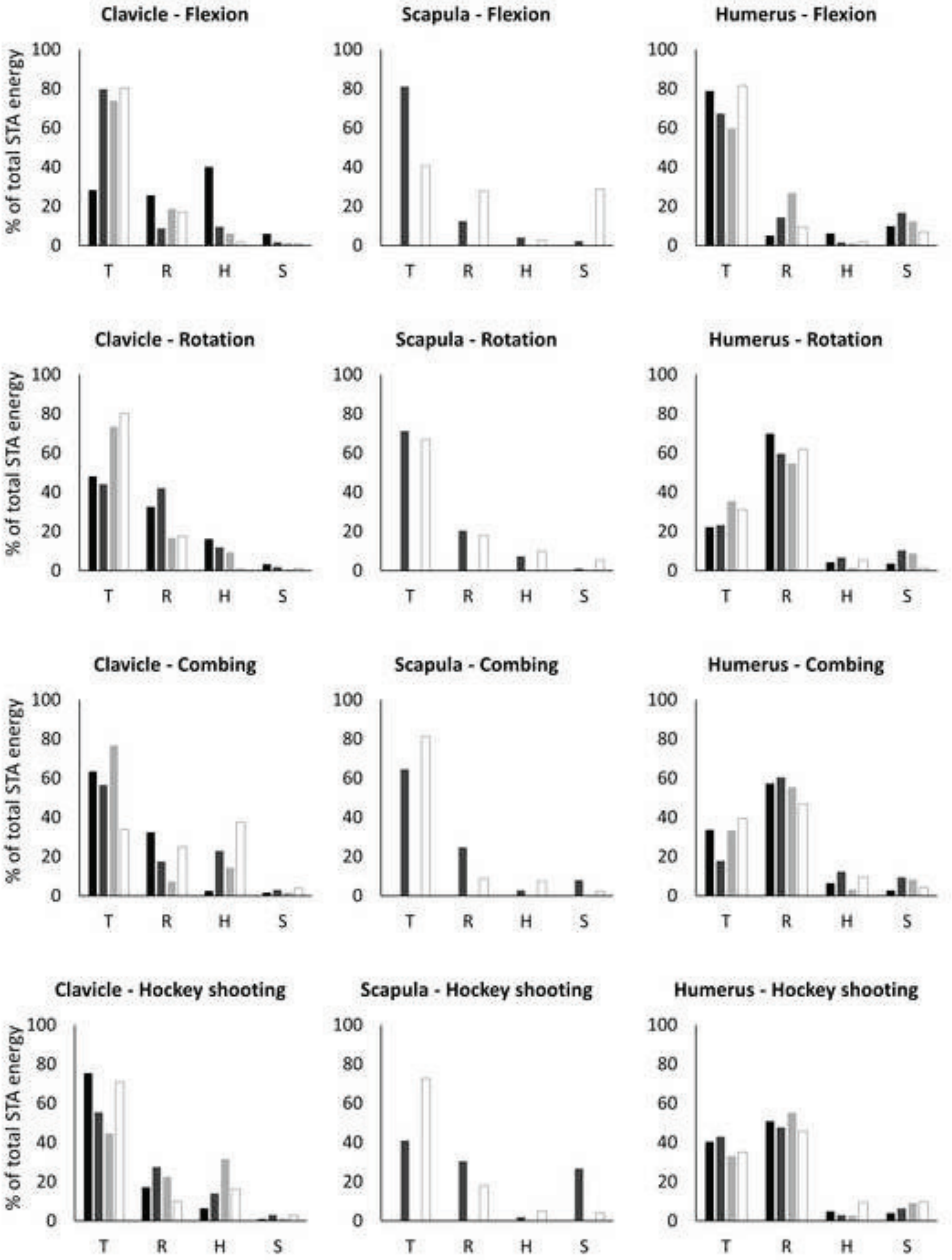
Clavicle - Flexion
Scapula - Flexion
Humerus - Flexion
Clavicle - Rotation
Scapula - Rotation
Humerus - Rotation
Clavicle - Combing
Scapula - Combing
Humerus - Combing
Clavicle - Hockey shooting
Scapula - Hockey shooting
Humerus - Hockey shooting
% of total STA energy
0
20
40
60
80
100
T
R
H
S